Available online at www.sciencedirect.com
SCIENCE DIRECT®
Journal of Solid State Chemistry 171 (2003) 434–438
JOURNAL OF SOLID STATE CHEMISTRY
http://elsevier.com/locate/jssc

$(ZrO_2)_{0.85}(REO_{1.5})_{0.15}$ (RE = Sc, Y) solid solutions prepared via three Pechini-type gel routes: 1—gel formation and calcination behaviors

Yawen Zhang, Ang Li, Zhengguang Yan, Gang Xu, Chunsheng Liao, and Chunhua Yan*

State Key Laboratory of Rare Earth Materials Chemistry and Applications & PKU-HKU Joint Lab on Rare Earth Materials and Bioinorganic Chemistry, College of Chemistry and Molecular Engineering, Peking University, Beijing 100871, China

Received 25 April 2002; received in revised form 8 September 2002; accepted 12 September 2002

Abstract

$(ZrO_2)_{0.85}(REO_{1.5})_{0.15}$ (RE = Sc, Y) nanoparticles with pure cubic fluorite structure have been synthesized by three Pechini-type gel routes, viz. poly(vinyl alcohol) containing-process (route I), poly(ethylene glycol) and formic acid-containing process (route II), and in situ polymerizable complex method (route III). The coordination modes between metal ions and polymers in the gels are shown to be highly correlative with the synthesis route used. The gels prepared by route III have the strongest coordination throughout their network and therefore the best chemical homogeneity. The altered variety of polymer and cross-linking within the gels adopted by these three routes has made the as-synthesized samples show appreciable differences in thermal behavior, powder reactivity and nanoparticle properties.

Keywords: Sc- or Y-doped zirconia; Gel syntheses; Gel formation; Calcination behaviors

1. Introduction

As a green energy source for the new century, solid oxide fuel cells (SOFCs) have stimulated continuing interest in recent years [1]. Yttria and scandia stabilized zirconia (YSZ, ScSZ) have been recognized as good candidate electrolytes of SOFCs operated at 700–1000°C due to their high oxide ion conductance [1]. Electrolytes with high performance are essential for the fabrication of commercial SOFCs with high-energy-converting efficiency and extended operating lifetime, and facilitate their processing into requisite parts in the form of dense or porous materials. Various synthetic methods have shown good potential to improve the properties of ceramic materials via tailoring the ceramic microstructures [2].

Previously, many techniques that use solid-state reactions [3], co-precipitations [4], hydrothermal syntheses [5], gel routes [6] and thermal decompositions of complex precursors [7] have been developed to prepare ceramic electrolytes. Among these methods, the gel route utilizes homogeneous precursors on a molecular level and thus enables the low-temperature synthesis of multicomponent oxide powders with the best homogeneity [8].

Although several gel routes have been exploited to synthesize YSZ, systematic studies of the effects of various synthesis routes on the microstructures and properties for a given electrolyte are scanty. Similarly, gel synthesis of ScSZ has not been investigated adequately. Therefore, it is worthwhile to reveal how the synthesis methods, particularly, various gel routes, affect the microstructures and performance of ceramic electrolytes such as ScSZ and YSZ.

More recently, our attention has focused on the exploration of the oxide ion conductance in the nanostructured $(ZrO_2)_{0.85}(REO_{1.5})_{0.15}$ (RE = Sc, Y) owing to their size-dependent properties [9]. In our latest article, we reported the influence of polymeric precursor compositions on the microstructure and the electrical properties of $(ZrO_2)_{0.85}(REO_{1.5})_{0.15}$, using one Pechini-type gel route [10]. In this work, we have used three Pechini-type gel routes to prepare $(ZrO_2)_{0.85}(REO_{1.5})_{0.15}$ (RE = Sc, Y) solid solutions. In the following section, the gel formation and calcination behaviors are presented.

*Corresponding author. Fax: +86-10-6275-4179.
E-mail address: chyan@chem.pku.edu.cn (C. Yan).

0022-4596/03/$ - see front matter © 2003 Elsevier Science (USA). All rights reserved.
doi:10.1016/S0022-4596(02)00227-X

2. Experimental

2.1. Preparation

Route I [11]: $ZrO(NO_3)_2$ [analytical reagent (AR), 20.4 mmol], $Sc(NO_3)_3$ [or $Y(NO_3)_3$] (AR, 3.6 mmol), and 1.32 g of poly(vinyl alcohol) (PVA) (degree of hydrolysis: 97%; degree of polymerization: 1750) were used to make the stock solution (60 mL) in a flask (100 mL). Upon heating in an oil bath, the PVA completely dissolved in the solution at 80–90°C. After being refluxed at 110°C for 30 min, the transparent solution became turbid and yellowish, indicating the formation of colloids. After a total reflux period of 24 h, the turbid stock solution turned highly viscous. On evaporation with an electric oven in open air, the viscous precursor swelled up to form yellow gel owing to the liberation of NO_x gases from the decomposed HNO_3. The gel was dried at 110°C for 8 h prior to calcination.

Route II [10]: $ZrO(NO_3)_2$ (AR, 20.4 mmol), $Sc(NO_3)_3$ [or $Y(NO_3)_3$] (AR, 3.6 mmol), formic acid (72 mmol), 3 g of poly(ethylene glycol) (PEG) (CP grade; molecular weight: 20,000) were taken to prepare the stock solution (60 mL) in a flask (100 mL). After being refluxed at 120°C for 1 h in an oil bath, the color of the stock solution gradually became yellowish, as HNO_3 decomposed with liberation of NO_x gases. After a total reflux period of 24 h, a transparent polymer precursor solution was formed. On evaporation with an electric oven in open air, the precursor became viscous, while further decomposition of HNO_3 occurred. The viscous liquid was then kept drying at 110°C for 8 h until yellow or white gel with swelled volume was yielded.

Route III (6, 12): $ZrO(NO_3)_2$ (AR, 20.4 mmol), $Sc(NO_3)_3$ [or $Y(NO_3)_3$] (AR, 3.6 mmol), 9.65 mL of ethylene glycol (AR, 174 mmol), 6.05 g of citric acid monohydrate (AR, 28.8 mmol) were utilized to fabricate the stock solution (60 mL) in a flask (100 mL). With the addition of citric acid, a white precipitate formed promptly. After being refluxed at 130°C for 24 h in an oil bath, a highly viscous and yellow solution formed. On further refluxing at 170°C for 0.5 h, the viscous solution was converted to a yellow solid substance, revealing the formation of the polymeric gel (resin). The substance was dried at 110°C for 8 h.

The dried gels were powdered using an agate pestle and mortar, and then calcined over 400–1000°C for 10 h in a muffle furnace in order to determine their calcination behaviors. In this work, the Sc- or Y-doped zirconia samples are referred to as SZ1 and YZ1 for route I, SZ2 and YZ2 for route II, and SZ3 and YZ3 for route III hereafter. The compositions of the dried gels were determined by elemental analysis. Found: C, 10.18%; H, 2.762%; N, 3.530% for SZ1. Found: C, 9.915%; H, 2.745%; N, 3.989% for YZ1. Found: C, 19.82%; H, 3.401%; N, 0.750% for SZ2. Found: C, 21.69%; H, 4.330%; N, 1.527% for YZ2. Found: C, 32.02%; H, 4.22%; N, 0.094% for SZ3. Found: C, 31.88%; H, 4.302%; N, 0.098% for YZ3.

2.2. Characterization methods

Elemental analysis of C, H and N was performed with a Carlo Erba 1102 elemental analyzer. FTIR spectra were measured by microscopic IR, using a Nicolet Magna 750 FTIR spectrometer in the range of 400–4000 cm^{-1}. The thermo-gravimetry and differential thermal analysis (TG-DTA) curves were recorded with a DuPont 2100 thermal analyzer in air at a heating rate of 10°C/min, using α-Al_2O_3 as a reference. The crystal structures were identified by a Rigaku D/max-2000 powder X-ray diffractometer, employing Cu$K\alpha$ radiation ($\lambda = 1.5408$ Å). The lattice parameters were calculated with least-squares methods. The average grain size was estimated according to the Scherrer equation. The BET specific surface area S_{BET} and pore volume (V_p) distribution were measured by nitrogen physisorption at 77.5 K, using an ASAP 2010 analyzer (Micromeritics Co. Ltd.). The pore size distribution was calculated from the adsorption branch of the isotherms, based on the BJH method [13]. The BJH pore diameter (r_p) was calculated as $4V_p/S_{BJH}$. Nanoparticle morphology was observed by transmission electronic spectroscopy (TEM, 200CX, JEOL).

3. Results and discussion

3.1. Characterization of the gel

XRD analyses in the 2θ range of 25–80° strongly suggested that all the gels prepared by the three routes have an amorphous structure.

In Fig. 1, we show the IR spectra of the as-synthesized gels. For all the gels, the strong peak within 1320–1380 cm^{-1} was ascribed to the uncoordinated nitrate ions [14]. In Fig. 1(a), the appearance of strong peaks at 1680 and 1553 cm^{-1} for SZ1, and 1672 and 1561 cm^{-1} for YZ1, reveals the existence of carboxyl groups in these gels. The two peaks could be ascribed to antisymmetric and symmetric stretching vibrations of coordinated carboxyl groups, respectively [15], and are absent from the IR spectrum of PVA. Therefore, it is considered that hydroxyl groups in PVA were partially oxidized to carboxyl functions by nitric acid during the gel formation in route I upon refluxing. In this case, the oxidization-derived carboxyl groups could combine with the metal ions to form polymeric complexes, which might result in white colloids and hence the phase separation, as observed in the experiment. On the other hand, the reduction of nitrate ions with liberation of NO_x gases made the reaction solution yellowish.

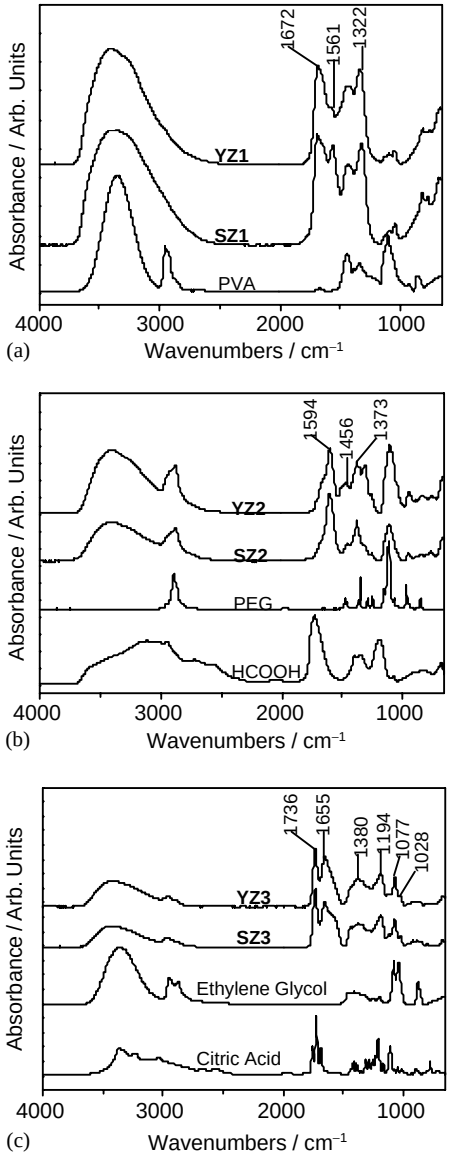

Fig. 1. IR spectra of the dried gels (SZ1, YZ1, SZ2, YZ2, SZ3 and YZ3), PVA, PEG, formic acid, citric acid and ethylene glycol.

Recently, we reported the IR spectra of the precursor solutions of Sc-doped zirconia prepared by route II [10]. We observed that refluxing of the precursor solution caused the reduction of the amount of nitric acid and the coordination between formic acid and metal ions. Hereby, as shown in Fig. 1(b), the emergence of two peaks at 1596 and 1447 cm^{-1} for SZ2 ($\Delta v = 149\,cm^{-1}$), and 1594 and 1456 cm^{-1} for YZ2 ($\Delta v = 148\,cm^{-1}$), can be attributed to antisymmetrical and symmetrical stretching modes for a bridging bidentate complex, respectively, formed by the coordination of formic acid with metal ions [15]. From Fig. 1(b), we also noted the stretching mode of carboxyl groups for free formic acid centers at 1724 cm^{-1}.

In this work, the characteristics of the gels produced from in situ polymerizable complex method (Pechini method) [12] are exemplified by the IR spectra of SZ3 and YZ3. In Fig. 1(c), the peaks at 1737, 1194 and 1028 cm^{-1} for SZ3, and 1736, 1194 and 1029 cm^{-1} for YZ3, are associated with the stretching modes of C═O, $–COO^-$ and –O–CH–, respectively, indicating the existence of esters in the gels, formed by esterification of citric acid with ethylene glycol [16]. The strong peak at 1694 cm^{-1} for SZ3 and 1694 cm^{-1} for YZ3 can be assigned to the antisymmetric $–COO^-$ stretching mode for an unidentate complex [16]. On the other hand, the absence of the band at 1728 cm^{-1} for the protonated –COOH group strongly suggests that all organic acid groups in the gels are combined either with ethylene glycol forming esters or with cations forming unidentate complexes, thus ensuring the immobilization of metal complexes in the rigid polymer matrix of SZ3 and YZ3.

Fig. 2 typically exhibits combined TG-DTA runs of the gels of SZ1, SZ2 and SZ3. The TG-DTA curves show that the decomposing processes for SZ1 and YZ1 gels are similar. First, the breakdown of the residual nitric acid occurs between 160°C and 240°C for SZ1, and between 160°C and 210°C for YZ1. Secondly, the cleavage of the organic components composed of PVA and the polymeric complexes takes place within

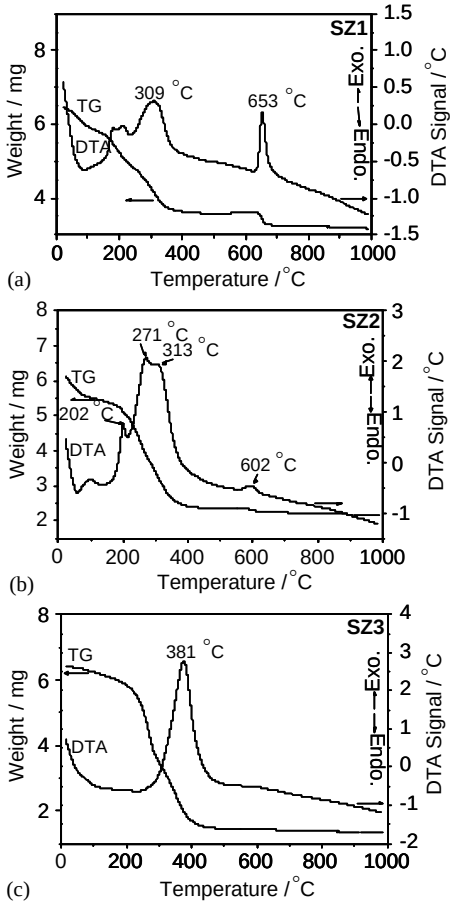

Fig. 2. Combined TG-DTA runs of the gels of (a) SZ1, (b) SZ2 and (c) SZ3.

240–370°C for SZ1, and within 310–410°C for YZ1. The burning of the organics leads to the appearance of a strong exothermic peak. Kwon et al. reported that nitrate ions and PVA decomposed at about 180°C and 400°C, respectively [11]. Finally, a strong exothermic effect was noticed at 653°C for SZ1 and 664°C for YZ1, which might be produced by the transition from an amorphous to the cubic crystalline structure during the gel decomposition [10].

The decomposition of SZ2 and YZ2 can be roughly divided into three steps. The first is the breakdown of the residual nitric acid at about 202°C and 191°C, respectively, giving a small exothermic peak. The second is the cleavage of the organic components composed of PEG, free formic acid and the corresponding complexes within 215–405°C for SZ2 and within 280–400°C for YZ2, accompanied by a very strong exothermic peak. Lastly, a small exothermic effect was noticed to center at 602°C for SZ2 and 536°C for YZ2, as a result of the transition from an amorphous to crystalline structure during the gel decomposition [10].

We observed that both SZ3 and YZ3 gels take on single step of decomposition and show a very strong exothermic peak, as was also observed by Yokota et al. [6]. The breakdown of the polymeric complexes arises over 300–500°C for SZ3 and YZ3, However, the thermal effect related to the phase transition from amorphous to crystalline may be masked by the above strong exothermic reaction.

As is discussed above, the gels prepared by routes I, II and III can completely decompose at temperatures below 410°C, 400°C and 500°C, respectively. Therefore, it is considered that the gels prepared by route III display the highest thermal stability, indicating that the strongest coordination exist in the gels prepared by this method. In the past, enhanced coordination throughout the gels was confirmed to reduce the mobility of metal ions, and thus prevent them from segregating during the gel formation [8]. Therefore, the immobilization of metal complexes in the rigid polymer network prepared by route III may make the SZ3 and YZ3 gels exhibit superior chemical homogeneity to the other samples.

3.2. Calcination behaviors

Fig. 3 displays the typical XRD patterns of SZ1, SZ2 and SZ3 calcined over 400–800°C in the 2θ range of 20–80°. For a given sample, the peak intensity increases with the calcination temperature, indicating that calcination at high temperature can help Sc- or Y-doped zirconia to acquire full crystallization. The SZ1 and YZ1 samples calcined at 400°C still remain amorphously. However, the SZ2, YZ2, SZ3 and YZ3 samples calcined at 400°C are poorly crystallized and show a cubic structure. Hence, it is concluded that routes II and III offer advantages in low-temperature synthesis of Sc- and Y-doped zirconia over route I. All the samples calcined beyond 400°C have been crystallized in pure cubic structure.

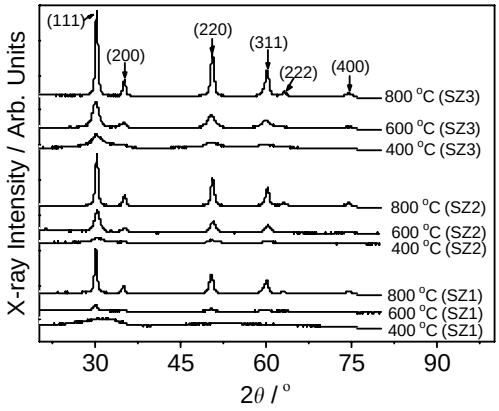

Fig. 3. XRD patterns of SZ1, SZ2, and SZ3 calcined over 400–800°C.

For the crystallized samples, the broadening of the diffraction peaks clearly reveals the formation of nanoparticles. In addition, the narrowing of the diffraction peak width with increasing calcination temperature shows that the crystallite size of the nanocrystals increases prominently with the temperature. Based on the Scherrer equation, values for the average grain size of the SZ1, YZ1, SZ2, YZ2, SZ3 and YZ3 samples calcined at 800°C were calculated as 24.8, 18.0, 21.9, 13.4, 23.3 and 13.5 nm, respectively. Average values of the lattice parameter, a, for Sc- or Y-dope zirconia samples calcined at 800°C were fitted to be at 5.10 and 5.14 Å, respectively.

For all the samples calcined over 400–1000°C, it is found that the higher the calcination temperature, the fewer the impurities. The total amount of the impurities attains less than 1% when calcined at 800°C. Therefore, the samples calcined at 800°C were selected for the investigation of the particle properties.

The BJH pore diameter, pore volume and the BET specific surface area are listed in Table 1. The BJH pore diameters and pore volumes of the samples are in the range of 12.4–24.4 nm and 0.0306–0.0602 cm^3g^{-1}, respectively, indicating that nanoparticles with mesoporous structure were built after calcining at 800°C [17], regardless of the synthesis route. Under the same conditions, the average pore diameter of Sc-doped zirconia nanocrystals is larger than that of Y-doped zirconia nanocrystals. From Table 1, we also observed that the S_{BET} values of the oxide powders derived from route II are higher than those prepared by routes I and III. The S_{BET} values of YZ1 and YZ3 are 1.6 times and double that of SZ1 and SZ3, respectively. However, the S_{BET} value of YZ2 is slightly smaller than that of SZ2.

By TEM, we observed that the nanoparticles of all the samples are in the range of 13–25 nm, and are tightly

Table 1
BJH[a] pore diameter r_p, pore volume V_p, and BET specific surface area S_{BET} of the gel-calcined oxide powders at 800°C

	SZ1	YZ1	SZ2	YZ2	SZ3	YZ3
r_p (nm)	19.5	13.3	9.0	6.57	24.4	12.4
V_p ($cm^3 g^{-1}$)	0.0306	0.0366	0.0602	0.0364	0.0445	0.0496
S_{BET} ($m^2 g^{-1}$)	6.6	10.7	24.2	20.1	7.6	15.5

[a] Ref. [13].

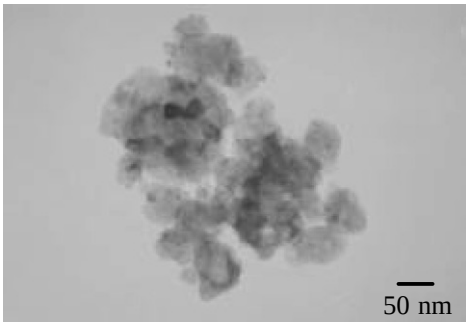

Fig. 4. TEM image of the SZ1 oxide powder calcined at 800°C.

agglomerated in lumps for minimizing the total surface or interfacial energy of the system after calcining at 800°C for 10 h. Representatively, Fig. 4 shows the TEM image for SZ1.

4. Conclusion

$(ZrO_2)_{0.85}(REO_{1.5})_{0.15}$ (RE = Sc, Y) nanoparticles with pure cubic fluorite structure were prepared by three Pechini-type gel routes. It is shown that the coordination modes between metal ions and polymers in the gels are highly correlative with the synthesis route. The strongest coordination throughout the gels and thus-obtained best chemical homogeneity are displayed by those prepared from the in situ polymerizable complex method. The altered variety of polymer and cross-linking within the gels adopted by the three routes have made the as-synthesized samples show appreciable differences in thermal behavior, powder reactivity and nanoparticle properties. To sum up, the three Pechini-type gel routes used in this research enable us to prepare pure phased $(ZrO_2)_{0.85}(REO_{1.5})_{0.15}$ (RE = Sc, Y) nanoparticles at low processing temperature, and show more advantages such as low cost, high simplicity and much lower toxicity.

Acknowledgments

Grants-in-aid from MOST of China (G1998061300), NSFC (Nos. 20171003, 29832010 & 20023005) and Founder Foundation of Peking University are gratefully acknowledged.

References

[1] S.P.S. Badwal, Solid State Ionics 143 (2001) 39.
[2] D. Segal, J. Mater. Chem. 7 (1997) 1297.
[3] D.W. Strickler, W.G. Carlson, J. Am. Ceram. Soc. 48 (1965) 286.
[4] G. Xu, Y.W. Zhang, C.S. Liao, C.H. Yan, Solid State Comm. 121 (2002) 45.
[5] G. Dell'Agli, G. Mascolo, J. Eur. Ceram. Soc. 20 (2000) 139.
[6] O. Yokota, M. Yashima, M. Kakihana, A. Shimofuku, M. Yoshimura, J. Am. Ceram. Soc. 82 (1999) 1333.
[7] Y.W. Zhang, J.T. Jia, C.S. Liao, C.H. Yan, J. Mater. Chem. 10 (2000) 2137.
[8] M. Kakihana, M. Yoshimura, Bull. Chem. Soc. Jpn. 72 (1999) 1427.
[9] Y.W. Zhang, S. Jin, Y. Yang, G.B. Li, S.J. Tian, J.T. Jia, C.S. Liao, C.H. Yan, Appl. Phys. Lett. 77 (2000) 3409.
[10] Y.W. Zhang, Y. Yang, S.J. Tian, C.S. Liao, C.H. Yan, J. Mater. Chem. 12 (2002) 219.
[11] S.W. Kwon, S.B. Park, G. Seo, S.T. Hwang, J. Nucl. Mater. 257 (1998) 172.
[12] M.P. Pechini, US Patent, July 11, No. 3330697, 1967.
[13] E.P. Barrett, L.G. Joyner, P.H. Halenda, J. Am. Chem. Soc. 73 (1951) 373.
[14] F. Pancrazi, J. Phalippou, F. Sorrentino, J. Zarzycki, J. Non-Cryst. Solids 63 (1984) 81.
[15] G.B. Deacon, R.J. Phillips, Coord. Chem. Rev. 33 (1980) 227.
[16] S.G. Cho, P.F. Johnson, R.A. Condrate Sr, J. Mater. Sci. 25 (1990) 4738.
[17] K.S.W. Sing, D.H. Everett, R.A.W. Haul, L. Moscou, R.A. Pierotti, J. Rouquerol, T. Siemieniewska, Pure Appl. Chem. 57 (1985) 603.